Available online at www.sciencedirect.com

ScienceDirect

IFAC Papers Online CONFERENCE PAPER ARCHIVE

IFAC-PapersOnLine 48-28 (2015) 1250–1255

# Identification of High-Tech Motion Systems: An Active Vibration Isolation Benchmark

**Robbert Voorhoeve,** * **Annemiek van Rietschoten,** *
**Egon Geerardyn,** ** **Tom Oomen** *

* *Eindhoven University of Technology. Department ME, CST group. Eindhoven, The Netherlands (e-mail: r.j.voorhoeve@tue.nl).*
** *Vrije Universiteit Brussel. Department ELEC. Brussels, Belgium.*

**Abstract:** The benchmark Active Vibration Isolation System (AVIS) in this paper is a complex high-tech industrial system used in vibration and motion control applications. The system is complex in the sense of high order flexible dynamics and multiple inputs and outputs. The aim of this benchmark is to compare different black box, linear time invariant system identification algorithms. Different large data sets are provided, enabling the use of both frequency domain and time domain identification approaches. The idea of the benchmark is to investigate both model accuracy and numerical reliability of the computational steps. Several reference solutions are provided, which demonstrate the challenging aspects of this benchmark already in the single-input single-output case. The benchmark data and additional info are available on the website of Tom Oomen [1].



## 1. INTRODUCTION

The aim of this Active Vibration Isolation System (AVIS) benchmark is to compare the capability of different black box, linear time invariant identification techniques to model complex industrial systems. The main idea is that an industrial high-tech system, characterized by highly accurate sensors & actuators, over-actuation and a high degree of active control, automatically constitutes a practically relevant setup on which to test identification algorithms. The presented benchmark system is complex in the sense of high order, lightly damped dynamics with a significant dimension in terms of inputs and outputs.

The proposed benchmark is based on a mechanical system that has applications in motion and vibration control. In the near future the requirements for motion and vibration control will become even tighter. To meet these future demands, it is envisaged in Oomen et al. (2014b, Section I.C) that active control of flexible dynamics is required, including the use of additional actuators and sensors and inferential control. This implies that the number of inputs and outputs is likely to increase, as well as the order of the relevant flexible dynamics. As a result, a model-based control approach (van de Wal et al., 2002) based on parametric models is a natural approach for a systematic control design for such complex multivariable systems.

Although many control applications for motion systems are reported in the literature, there is a strong indication that the modeling task still poses a major challenge. System identification is the natural approach for such systems, since it is inexpensive, fast, and accurate due to the almost infinite freedom in the design of experiments. However, there are indications that it is unclear for practitioners what method to prefer and choose from the large amount of approaches available.

These indications are at least threefold. First, most motion systems are still tuned manually using non-parametric models, see Van de Wal et al. (2002), Butler (2011). Second, it is explicitly indicated in earlier overviews of the motion control field, e.g., already in Steinbuch and Norg (1998, Section 4.2, limitations of tools), that modeling tools are not readily available. Third, besides the fact that many system identification approaches with different criteria have been developed, a significant number of results addressing issues with the numerical implementation of these methods have been developed, including frequency scaling (Pintelon and Kollár, 2005), amplitude scaling (Hakvoort and Van den Hof, 1994), the use of classical orthonormal polynomials and orthogonal rational functions (Heuberger et al., 2005, Section 3.1), (Ninness et al., 2000), (Ninness and Hjalmarsson, 2001), and more recently the use of orthonormal basis functions with respect to a discrete data-based inner product (Bultheel et al., 2005), (Van Herpen et al., 2014). Related numerical issues are also seen in subspace identification, see e.g., Verdult et al. (2002) and Chiuso and Giorgio (2004).

The proposed benchmark system is an Active Vibration Isolation System (AVIS), which is selected for its application interest, applicability and relevance, and challenge. Regarding application interest, these systems are used in diverse fields, ranging from precision equipment such as lithography and scanning tunneling and atomic force microscopy to vehicles, and their control is an active research topic by itself, see e.g., Landau et al. (2013). Regarding applicability and relevance, the considered AVIS is open-loop stable. This is in sharp contrast to typical high-performance motion systems that require closed-loop operation to stabilize the rigid-body behavior. As such, the approach eliminates issues that could arise due to closed-loop operation, including potential bias and the influence of the controller on the resulting model, enabling a meaningful and unambiguous evaluation of many available identification approaches. Regarding the challenge component, the system has 8 inputs and 6 outputs with high-order flexible dynamics over a large dynamic range, leading to a

[1] `http://www.dct.tue.nl/toomen/avis/avis.html`

2405-8963 © 2015, IFAC (International Federation of Automatic Control) Hosting by Elsevier Ltd. All rights reserved.
Peer review under responsibility of International Federation of Automatic Control.
10.1016/j.ifacol.2015.12.303

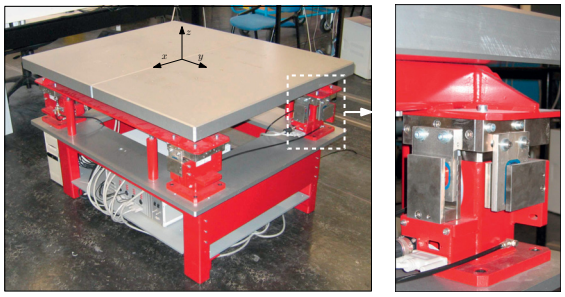

Fig. 1. Benchmark AVIS and isolator configuration.

complex identification problem, e.g. compared to related control benchmarks in this field (Landau et al., 2013). It is emphasized that though significantly challenging, it is expected that future motion systems have a much higher complexity. In this respect the AVIS is a good compromise between e.g. the applicability in the sense of open-loop operation and the challenge component in the sense of problem complexity.

The main challenge lies in obtaining a parametric model of the system, both in terms of model accuracy and numerical reliability. In view of the control application, the typical approach is via the frequency domain. The main reason is that, in addition to the arguments provided in Pintelon and Schoukens (2012), the resulting controller is often evaluated in the frequency domain using Bode and Nyquist diagrams, providing a highly preferred controller validation step in industrial control engineering. Still, given the close relations between the time domain and the frequency domain, it would be very interesting to compare approaches in both domains regarding performance and numerical reliability. In addition, given the often pursued frequency domain approach, this also leads to a second sub-challenge of the provided benchmark setup: the efficient and accurate non-parametric identification of such lightly damped systems with many inputs and outputs.

## 2. THE SETUP

The benchmark setup is an Active Vibration Isolation System (AVIS) built by IDE (Integrated Dynamics Engineering). It is shown in Figure 1. The AVIS consists of an aluminum table suspended on air mounts. It is equipped with eight actuators, two at each corner (see Figure 1), and six sensors, also two at each corner apart from one.

The actuators, shown in Figure 1, are voice-coil or Lorentz actuators (Munnig Schmidt et al., 2011, Section 5.2). These actuators are characterized by a highly linear relation between the applied current and the resulting force.

The sensors are geophones (Munnig Schmidt et al., 2011, Section 8.7.2). These are inertial sensors that are designed to measure the absolute velocity of the system with respect to an inertial reference frame, instead of relative to the floor. Such an absolute measurement is particularly useful in vibration isolation since it enables skyhook damping (Karnopp, 1995), which is explained on the next page in the textbox on vibration isolation.

The system is located on an isolated floor segment in our lab to reduce the effects of external disturbances on the measurements. The measurement setup that is used for this system is a zero-order hold setup. The transfer function that is measured in this setup, is the transfer function from the predetermined, discrete and noiseless generator signal $u_d(n)$ to the sampled, noisy output measurement $y(nT_s)$. The data acquisition card in this setup, is a Quanser Q8 and the experiments are performed using Simulink Real-Time™. No anti-aliasing filters are used in this setup, which for a zero-order hold measurement setup is the conventional configuration (Pintelon and Schoukens, 2012, Section 13.3).

## 3. MEASUREMENT

Measurements of the benchmark system are performed using multisine excitations as well as normally distributed zero-mean white noise. These types of excitation signals are both frequently used in system identification and enable identification of the system in a wide frequency range. The noise sequences are defined as

$$u_{\text{noise}}(n) \sim \mathcal{N}(0, \sigma). \tag{1}$$

The multisine signals are defined as

$$u_{\text{MS}}(n) = \sum_{k=1}^{K} A_k \sin(2\pi k n/N_p + \phi_k), \tag{2}$$

where $N_p$ is the total number of points in one period of the signal. The phases $\phi_k$ are sampled from a uniform distribution over $[0, 2\pi]$. The amplitudes $A_k$ are chosen such that only the odd frequency bins, $k = 1, 3, 5, \ldots$ are excited. For these odd frequencies, the amplitude $A_k$ is constant, normalized such that the total rms of the input signal is equal to 1/6 Volt.

To perform MIMO multisine measurements of the benchmark system, full random orthogonal multisines are used (Pintelon and Schoukens, 2012, Section 3.7). Here, a $n_u \times n_u$ (where $n_u$ is the number of inputs) matrix of input signals is constructed in frequency domain as

$$\mathbf{U}(k) = D_U(k) T D_\phi(k), \tag{3}$$

where $D_U(k)$ is a complex diagonal matrix containing the amplitudes and phases for $n_u = 8$ independently generated random phase multisine signals, $T$ is a suitably chosen orthogonal matrix and $D_\phi(k)$ is a complex diagonal matrix containing random phase sequences, leading to independent columns of $\mathbf{U}(k)$. This extra randomness is necessary when the system exhibits (weakly) nonlinear behavior, for more details see Pintelon and Schoukens (2012, Section 13.3). In (3), the following definition of the DFT is used

$$X(k) = \frac{1}{\sqrt{N}} \sum_{n=0}^{N-1} x(nT_s) e^{-j2\pi nk/N}. \tag{4}$$

For the multisine measurements, each of the columns of $\mathbf{U}(k)$ represents a different experiment that is performed ($N_{\text{exp}} = n_u$) and the rows correspond to the input channels to which that signal is applied. The construction of the input matrix as in (3), ensures that the input matrix can be inverted in a numerically reliable way.

The multisine signals are applied periodically. For all experiments $P = 15$ periods are measured with a period length of $T_p = 10$ seconds and with a sampling frequency of 20 kHz. Furthermore, to quantify and diminish the influence of the stochastic nonlinear contributions on the measurements (using the robust method (Pintelon and Schoukens, 2012, section 4.3)), $M = 15$ independently generated realizations of the full random orthogonal multisines are measured. For the measurements using Gaussian

**Vibration isolation** aims to suppress the influence of external disturbances on the payload. These external disturbances can be separated in two classes, $F_{d1}$, acting on the floor and $F_{d2}$, acting directly on the payload. See Fig. 3 for a schematic model of the AVIS.

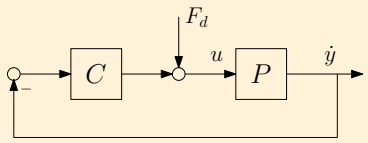


Fig. 2. Simple feedback interconnection for active vibration isolation.

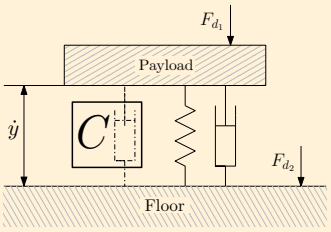


Fig. 3. Traditional setup, measuring the velocity relative to the floor.

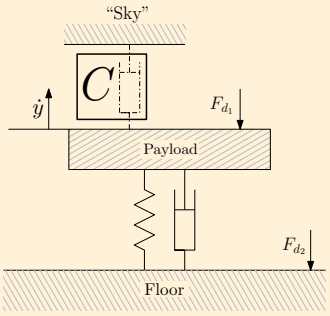


Fig. 4. Skyhook damping of the AVIS, using an absolute velocity measurement.

In passive vibration isolation the challenge is to design suspension characteristics (modeled by a spring and damper in Fig. 3), such that the disturbances $F_{d1}$ and $F_{d2}$ are optimally suppressed. To suppress the floor disturbances $F_{d2}$, a soft suspension is desired since this maximizes the frequency range in which the floor and AVIS are decoupled, leading to good isolation of the AVIS with respect to floor disturbances. However, to suppress the system disturbances $F_{d1}$, a stiff suspension is desired because this minimizes the deflection caused by such a disturbance. Hence, there is a clear trade-off in passive vibration isolation.

In active vibration isolation, the suppression of external disturbances is enhanced through active feedback control, see Fig. 2. One possibility is to measure and actively control the velocity of the system with respect to the floor, as shown in Fig. 3. In this configuration however, the controller can be interpreted as an extra suspension element between the floor and the AVIS. This means the same trade-off as in passive vibration isolation exists between the suppression of $F_{d1}$ and $F_{d2}$.

If a measurement is available of the absolute velocity of the system, so-called skyhook damping can be used. The name skyhook damping references the interpretation of the controller as a suspension element (damper) between the AVIS and the fixed world or "sky", see Fig. 4. This effectively eliminates the trade-off between the suppression of floor disturbances and suppression of system disturbances, since they are both suppressed by a strong coupling between the AVIS and the (disturbance free) fixed world. In this case, a high control bandwidth is thus desired to attenuate both $F_{d1}$ and $F_{d2}$.

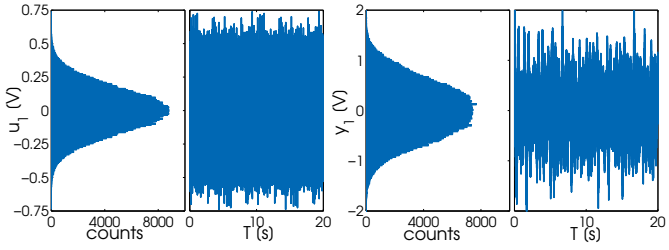


Fig. 5. Timeseries and histograms of two periods of multisine input and an output signals.

noise sequences as inputs, again an $n_u \times n_u$ input matrix is constructed as in (3), however the initial $n_u = 8$ frequency domain signals which define $D_U(k)$ are the Fourier coefficients of the Gaussian noise sequences instead of the multisines. For each of the noise experiments, the excitation signals were applied for 300 seconds. For an overview, see Table 1.

In Figure 5, the time-series and histograms are shown of the first input and output for two periods of the multisine excitation. From these figures, it can be seen that the amplitude distribution of the multisine signals approximates a Gaussian distribution, which is due to the use of random phases.

Figure 6 shows the frequency domain spectra of the same input and output data as seen in Figure 5. The input spectrum clearly equals the designed deterministic amplitude spectrum for the excited frequencies and shows no excitation for the non-excited frequencies. The output spectrum already reveals some of the system's amplitude behavior and confirms that the system contains a large

Table 1. Overview of conducted experiments.

| | $N_{\text{exp}}$ | real. $M$ | periods $P$ | $T_{\text{p}}$ $[s]$ | $T_{\text{tot}}$ $[s]$ |
|---|---|---|---|---|---|
| Multisine | 8 | 15 | 15 | 10 | 18000 |
| Noise | 8 | 1 | 1 | 300 | 2400 |

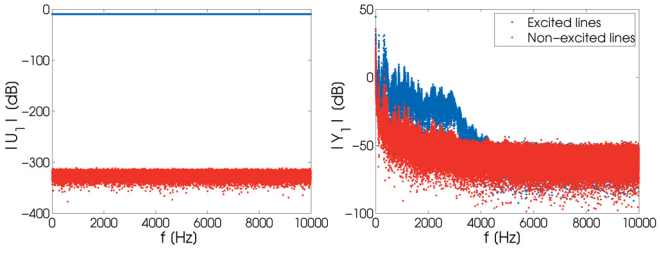


Fig. 6. Frequency domain amplitudes of two periods of multisine input and an output signals

number of lightly damped modes, which will become clear in Figure 7. The output spectrum also shows a distinction between the excited and non-excited lines, however this distinction is not as sharp as in the input spectrum. This can be attributed to measurement noise and non-linearities in the system. Next, a non-parametric characterization of the frequency response of the system is performed to reduce and quantify the influence of these phenomena.

## 4. NON-PARAMETRIC IDENTIFICATION

As an intermediate step in system identification, a non-parametric model can be used. This provides valuable insight in the system behavior and also provides a means for data reduction. In this section, the frequency response matrix of the system is estimated using the multisine measurements described in section 3.

Real-life systems will always exhibit some non-linear behavior, therefore the frequency response matrix will at best be a linear approximation of the system behavior. To obtain a good linear approximation, the so-called robust method for estimating the best linear approximation is used, see Pintelon and Schoukens (2012, Sections 4.3.1 & 7.3.6). Note that this best linear approximation can still depend on certain aspects of the applied input signal such as its rms value and DC offset. Here, a self-contained summary of this method for estimating the best linear approximation is described.

For each realization $m$, experiment $e$ and period $p$, a $n_y \times 1$ vector of output signals (with signal length $N = f_s T_p$) is measured. These are first transformed to the frequency domain using the DFT defined by (4). The output observations are described by

$$Y(k) = G_{\mathrm{BLA}}(\Omega_k)U(k) + V_Y(k) + Y_s(k) + T_Y(\Omega_k), \quad (5)$$

where $G_{\mathrm{BLA}}(\Omega_k)$ is the best linear approximation of the system, $U(k)$ is the DFT of the input signal, $V_Y(k)$ is the disturbing noise on the output observations, $Y_s(k)$ is the stochastic non-linear contribution and $T_Y(\Omega_k)$ is the transient response (or leakage) term. The influence of all three of these disturbance terms should be mitigated and/or quantified during non-parametric identification.

The transient term $T_Y(\Omega_k)$ is mitigated by discarding the measurement data from the first $P_t = 5$ periods of the multisine measurements. Next, the frequency domain signals are averaged over the remaining $P_{\mathrm{ss}}$ steady-state periods, to mitigate the influence of $V_Y(k)$

$$\hat{Y}^{[m,e]}(k) = \frac{1}{P_{\mathrm{ss}}} \sum_{p=P_t+1}^{P} Y^{[m,e,p]}(k). \quad (6)$$

To quantify the remaining influence of this noise term, the covariance of $\hat{Y}^{[m,e]}(k)$ is determined from

$$\hat{C}_{\hat{Y}}^{\text{noise }[m,e]}(k) = \frac{1}{P_{\mathrm{ss}}(P_{\mathrm{ss}}-1)} \sum_{p=P_t+1}^{P} e_Y^{[m,e,p]}(k) e_Y^{[m,e,p]^H}(k), \quad (7)$$

with

$$e_Y^{[m,e,p]}(k) = Y^{[m,e,p]}(k) - \hat{Y}^{[m,e]}(k). \quad (8)$$

Averaging over the multisine periods does not mitigate the influence of the stochastic non-linear contributions since they have the same periodicity. Therefore, to mitigate and quantify the influence of $Y_s(k)$, an averaging step over the different realizations $m$ is performed. Since the phases of the input sinusoids for the different realizations vary, these varying phases first need to be eliminated before a meaningful average over the realizations can be computed. This is done by first relating the output signals $\hat{Y}^{[m,e]}(k)$ to the inputs signals. The signals of the $n_u$ experiments are combined to form the following matrix of outputs

$$\hat{\mathbf{Y}}^{[m]}(k) = \left[\hat{Y}^{[m,1]}(k)\ \hat{Y}^{[m,2]}(k)\ \ldots\ \hat{Y}^{[m,n_u]}(k)\right]. \quad (9)$$

The matrix of input signals $\mathbf{U}^{[m]}(k) \in \mathbb{C}^{n_u \times n_u}$ (see (3)) is written as:

$$\mathbf{U}^{[m]}(k) = D_{|U|}(k) T_{\angle U}^{[m]}(k) \quad (10)$$

where $D_{|U|}(k)$ is a diagonal matrix containing amplitude information of the input signal and $T_{\angle U}^{[m]}(k)$ is a unitary matrix containing all the phase information of the input signals, obtained by rewriting (3) in phasor notation. This unitary matrix is used to relate the output signals to the input signals, allowing the computation of a meaningful average over the $M$ independent realizations, i.e.,

$$\hat{\mathbf{Y}}_U^{[m]}(k) = \hat{\mathbf{Y}}^{[m]}(k) T_{\angle U}^{[m]^H}(k), \quad (11)$$

$$\hat{\mathbf{Y}}_U(k) = \frac{1}{M} \sum_{m=1}^{M} \hat{\mathbf{Y}}_U^{[m]}(k). \quad (12)$$

Next the covariance of this estimate is computed using

$$\hat{C}_{\hat{Y}_U}^{[e]}(k) = \frac{1}{M(M-1)} \sum_{m=1}^{M} r_Y^{[m,e]}(k) r_Y^{[m,e]^H}(k), \quad (13)$$

with

$$r_Y^{[m,e]}(k) = \hat{\mathbf{Y}}_{U\,[:,\,e]}^{[m]}(k) - \hat{\mathbf{Y}}_{U\,[:,\,e]}(k). \quad (14)$$

The previously obtained covariance estimates of the noise are used to estimate the noise covariance on $\hat{\mathbf{Y}}_U(k)$

$$\hat{C}_{\hat{Y}_U}^{\text{noise }[e]}(k) = \frac{1}{M^2} \sum_{m=1}^{M} \hat{C}_{\hat{Y}}^{\text{noise }[m,e]}(k). \quad (15)$$

Finally the best linear approximation is computed through

$$\hat{G}_{\mathrm{BLA}}(\Omega_k) = \hat{\mathbf{Y}}_U(k) D_{|U|}^{-1}(k). \quad (16)$$

One final averaging step over the $n_u$ experiments yields

$$\hat{C}_{\hat{Y}_U}(k) = \frac{1}{n_u} \sum_{e=1}^{n_u} \hat{C}_{\hat{Y}_U}^{[e]}(k), \quad (17)$$

and

$$\hat{C}_{\hat{Y}_U}^{\text{noise}}(k) = \frac{1}{n_u} \sum_{e=1}^{n_u} \hat{C}_{\hat{Y}_U}^{\text{noise }[e]}(k). \quad (18)$$

The total and noise covariances of $\hat{G}_{\mathrm{BLA}}$ are computed by

$$\hat{C}_{\hat{G}_{\mathrm{BLA}}} = \mathrm{cov}(\mathrm{vec}(\hat{G}_{\mathrm{BLA}})) \approx \left(\overline{\mathbf{U}(k)\mathbf{U}^H(k)}\right)^{-1} \otimes \hat{C}_{\hat{Y}_U}(k), \quad (19)$$

where $\mathrm{vec}(\cdot)$ denotes the vectorization operator, and

$$\hat{C}_{\hat{G}_{\mathrm{BLA}}}^{\text{noise}} \approx \left(\overline{\mathbf{U}(k)\mathbf{U}^H(k)}\right)^{-1} \otimes \hat{C}_{\hat{Y}_U}^{\text{noise}}(k). \quad (20)$$

The results of this procedure for the first $2 \times 2$ subset of the benchmark setup are shown in Figure 7, showing the resulting best linear approximation as well as the total and noise standard deviations. These results show that a good signal to noise ratio ($> 10$dB) is achieved for a large frequency range and also clearly show the high order lightly damped dynamics of the system.

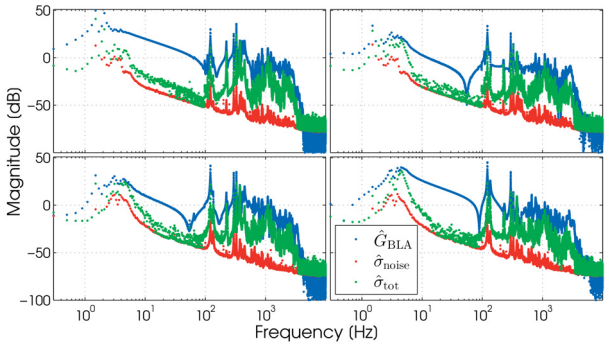


Fig. 7. Magnitude plots for the first $2 \times 2$ subset of the non-parametric estimate of $\hat{G}_{\mathrm{BLA}}$ for the AVIS, including the total and noise variances ($\hat{\sigma}_{\mathrm{tot}}$, $\hat{\sigma}_{\mathrm{noise}}$ respectively).

## 5. THE BENCHMARK CHALLENGE

### 5.1 Main benchmark challenge

The main benchmark challenge of this paper is to accurately fit a parametric model to the estimated frequency response function (or directly to the time-domain data). A number of metrics are formulated to assess the performance of different identification routines.

**Accuracy metric** To assess the accuracy of the obtained model, the value of the sampled maximum likelihood cost function is used, which is defined as:

$$V_{\mathrm{ML}}(\tilde{G}) = \sum_{k=1}^{m} \left[ \varepsilon_{\hat{G}_{\mathrm{BLA}}}(\Omega_k, \tilde{G})^H W(k) \varepsilon_{\hat{G}_{\mathrm{BLA}}}(\Omega_k, \tilde{G}) \right]^2, \tag{21}$$

where $\varepsilon_{\hat{G}_{\mathrm{BLA}}}(\Omega_k, \tilde{G})$ is given by

$$\varepsilon_{\hat{G}_{\mathrm{BLA}}}(\Omega_k, \tilde{G}) = \mathrm{vec}(\hat{G}_{\mathrm{BLA}}(\Omega_k) - \tilde{G}_{\mathrm{prop}}(\Omega_k)), \tag{22}$$

and the weight matrix is defined as

$$W(k) = \hat{C}^{-1}_{\hat{G}_{\mathrm{BLA}}}(k). \tag{23}$$

In (22), $\tilde{G}_{\mathrm{prop}}(\Omega_k)$ is the linear system (evaluated at frequency $k$) that results from a proposed identification routine. In this cost function the identified models are compared with the non-parametric BLA, ideally one would want to compare the identified models with the true model. A true model is however not available and therefore this non-parametric BLA which is estimated based on the full data-set is used instead.

**Subsets** The cost function (21) is specified for the full $6\times8$ MIMO case, but it can readily be reformulated such that a subset of the MIMO problem is considered. Since the full MIMO case is rather challenging, it is useful to first assess the performance of identification algorithms on SISO and smaller MIMO parts of the system before attempting the full MIMO case. The subsets that are considered for the benchmark are those using the first $[1:n_{y,\mathrm{id}}]$ output and the first $[1:n_{u,\mathrm{id}}]$ input channels. It should always be clearly indicated how many inputs and outputs are used.

**Numerical reliability** To assess the numerical reliability of the different identification algorithms, the condition number with respect to $L^2$ (denoted as $\kappa$) is used. Most identification methods solve a linear system of equations to calculate the fitting parameters or use a matrix decomposition such as SVD or QR as central solution step. The condition number for this central solution step is considered for this benchmark. For iterative algorithms the minimum, maximum and geometric mean values over all iterations should be mentioned.

**Other metrics** Additional relevant metrics are the computation time (and on what type of machine), to assess the efficiency of the method, and the order (McMillan degree) of the estimated model as well as the number of model parameters that were estimated. Table 2 shows an example of all the performance metrics for the reference solutions used in this paper.

### 5.2 Secondary benchmark challenge

As a secondary benchmark, a non-parametric identification challenge is formulated. The non-parametric identification solution shown in section 4 is used as a reference case. The challenge is to use the least amount of measurement data while maintaining a comparable model quality.

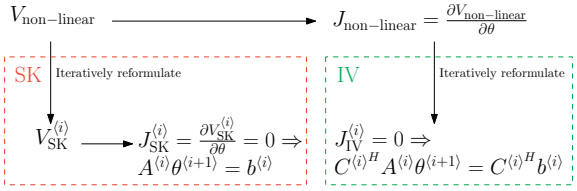


Fig. 8. Graphical depiction of the basic principles behind the applied SK and IV algorithms.

For example, local modeling techniques (LPM/LRM, see e.g., Geerardyn et al. (2014)) can be used to mitigate the transient response instead of discarding the measurement data from the first five periods, reducing the total amount of measurement periods required.

To quantify the model quality, the same cost function is used as in the parametric identification benchmark of Section 5, except a non-parametric $\tilde{G}_{\mathrm{prop}}(\Omega_k)$ is used instead of a parametric model. This cost function is only defined on a discrete frequency grid (see eq. (21)), but for this non-parametric benchmark, a subset of this frequency grid can be used. The cost function should then be normalized with the total number of frequency bins that are considered. If an entirely different frequency grid is obtained then the applied interpolation method should be clearly defined.

## 6. A REFERENCE SOLUTION

In this section, a reference solution is provided for the benchmark challenge where the first SISO element of the system is considered. This facilitates presentation and already reveals the challenging numerical aspects involved in the benchmark challenge. For the SISO case, the sampled maximum likelihood cost function (21) reduces to

$$V_{\mathrm{ML}\,i,j}(\theta) := \sum_{k=1}^{m} \left| \frac{\hat{G}_{\mathrm{BLA}\,i,j}(\Omega_k) - \tilde{G}(\Omega_k, \theta)}{\hat{\sigma}_{\hat{G}_{\mathrm{BLA}\,i,j}}(\Omega_k)} \right|^2, \tag{24}$$

where

$$\tilde{G}(\Omega, \theta) = \frac{N(\Omega, \theta)}{D(\Omega, \theta)}, \tag{25}$$

and where $N(\Omega, \theta)$ and $D(\Omega, \theta)$ are polynomials in the indeterminate $\Omega$. This cost function is non-linear in the parameters $\theta$.

Two different algorithms are utilized, the Sanathanan-Koerner (SK) algorithm (Pintelon and Schoukens, 2012, Section 9.8.3) and the Instrumental Variable (IV) algorithm (Blom and Van den Hof, 2010). As is shown in Figure 8, these approaches both involve solving a sequence of linear systems of equations. Note that these approaches need not converge monotonically, thereby providing additional robustness with respect to local minima.

The problem matrices of these algorithms ($C, A$ and $b$ as in Figure 8) depend on the particular parametrization of (25). Here, the following parametrizations are considered:

**Mon** monomials;

**ScM** monomials that are scaled such that the columns of $A$ and $C$ have a unity 2-norm; and

**BP** block polynomials $\phi_i$, $\psi_j$ that are bi-orthogonal with respect to the bi-linear form $\langle \psi_i, \phi_j \rangle_{C,A}$, that theoretically yield $\kappa(C^H A) = 1$ as introduced by Van Herpen et al. (2014).

Table 2. Benchmark criteria for reference solutions.

| Approach | $\min(V_{\mathrm{ML1,1}})$ | $\kappa_{\mathrm{min/gmean/max}}$ | $t_{\mathrm{comp}}$ [s] @i5-4670 | order/ $N_{\mathrm{par}}$ |
|---|---|---|---|---|
| IV,BP | 4.6e5 | 1/2/4e22 | 363 | 100/200 |
| IV,ScM | 5.4e5 | 2e17/2e18/3e19 | 165 | 100/200 |
| IV,Mon | 1.3e6 | 9e70/1e154/1e293 | 231 | 100/200 |
| SK,ScM | 1.5e6 | 5e9/2e15/6e16 | 168 | 100/200 |

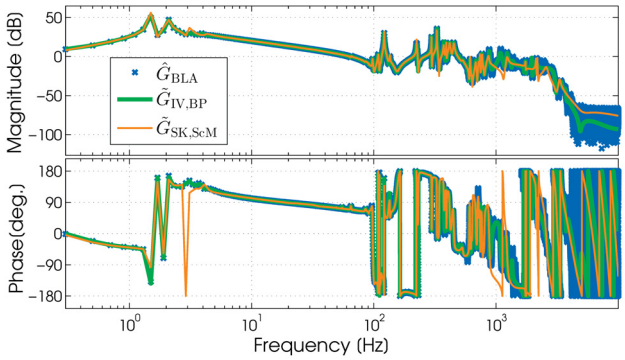


Fig. 9. Fitted models using the IV algorithm with a bi-orthonormal basis ($\tilde{G}_{\mathrm{IV,BP}}$) and the SK algorithm with scaled monomials ($\tilde{G}_{\mathrm{SK,ScM}}$).

In Figures 9 and 10 and Table 2 the results for these reference solutions of the SISO benchmark problem are shown. In Figure 10 it can be seen that only the IV algorithm parameterized with the bi-orthonormal basis functions converges within 200 iterations. All the other parametrizations used with the IV algorithm have much higher condition numbers which clearly influences the convergence properties of the algorithm. For the bi-orthonormal basis the condition number is equal to 1 for most iterations, however at some iterations it spikes, likely due to implementation issues with the algorithm that constructs these bases. That these numerical issues are already present for the SISO case shows the challenging numerical aspects involved in this benchmark.

## 7. DISCUSSION AND OUTLOOK

In this paper, a benchmark is presented which can be used to evaluate LTI system identification techniques on a complex industrial motion system with high order lightly damped dynamics. To assess the performance of available and future approaches in the field of linear system identification, evaluation criteria for model quality as well as numerical reliability are formulated. The criterion used to assess model accuracy is the sampled maximum likelihood cost function defined in (21). To assess the numerical reliability of the identification algorithms, the condition number of the central estimation step is used. The reference solution included in this paper shows the challenging numerical aspects involved in this benchmark.

The benchmark challenge in this paper is focused on the accurate and reliable identification of a nominal model for an industrial system. The ultimate goal of the system and hence the model is subsequent control design. The control goal introduces additional interesting aspects that may be of relevance for future investigation, including

- identification for control using control-relevant criteria;
- uncertainty identification for robust control, preliminary ideas have revealed interesting aspects, see Geerdyn et al. (2014); Oomen et al. (2014a), and Friedman and Khargonekar (1995) for related work;
- enforcing constraints, such as stability of models; and
- parametric disturbance modeling for disturbance-based control design.

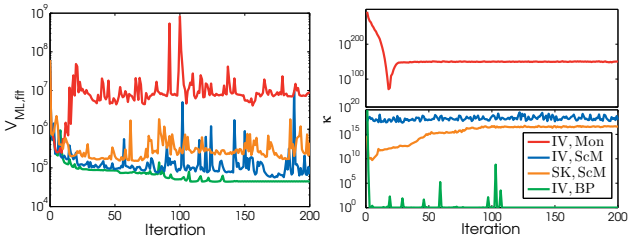


Fig. 10. Cost function values and conditions numbers during iterations for the reference solutions.

ACKNOWLEDGEMENTS

The authors want to thank Johan Schoukens and Maarten Steinbuch for the fruitful discussions. This research is supported by the TU/e Impuls program and ASML research as well as the Innovational Research Incentives Scheme under the VENI grant "Precision Motion: Beyond the Nanometer" (no. 13073) awarded by NWO and STW and by the Flemish Government (Methusalem) and by the Belgian Government through the IAP VII/19 (DYSCO) Program.

REFERENCES

Blom, R. and Van den Hof, P. (2010). Multivariable frequency domain identification using IV-based linear regression. In *Proc. CDC*, 1148–1153. Atlanta, GA.

Bultheel, A., van Barel, M., Rolain, Y., and Pintelon, R. (2005). Numerically robust transfer function modeling from noisy frequency domain data. *IEEE Trans. Automat. Contr.*, 50(11), 1835–1839.

Butler, H. (2011). Position control in lithographic equipment an enabler for current-day chip manufacturing. *IEEE Contr. Syst. Mag.*, 31(5), 28–47.

Chiuso, A. and Giorgio, P. (2004). On the ill-conditioning of subspace identification with inputs. *Automatica*, 40(4), 575–589.

Friedman, J.H. and Khargonekar, P.P. (1995). Application of identification in $\mathcal{H}_\infty$ to lightly damped systems: Two case studies. *IEEE Trans. Contr. Syst. Techn.*, 3(3), 279–289.

Geerardyn, E., Oomen, T., and Schoukens, J. (2014). Enhancing $\mathcal{H}_\infty$ norm estimation using local LPM/LRM, modeling: Applied to an AVIS. In *IFAC 19th Triennial World Congress*, 10856–10861. Cape Town, South Africa.

Hakvoort, R.G. and Van den Hof, P.M.J. (1994). Frequency domain curve fitting with maximum amplitude criterion and guaranteed stability. *Int. J. Contr.*, 60(5), 809–825.

van Herpen, R., Oomen, T., and Steinbuch, M. (2014). Optimally conditioned instrumental variable approach for frequency-domain system identification. *Automatica*, 50(9), 2281–2293.

Heuberger, P., Van den Hof, P., and Wahlberg, B. (2005). *Modelling and Identification with Rational Orthogonal Basis Functions*. Springer-Verlag London Ltd.

Karnopp, D. (1995). Active and semi-active vibration isolation. *Trans. ASME*, 117, 177–185.

Landau, I., Castellanos Silva, A., Airimitoaie, T.B., Buche, G., and Noë, M. (2013). Benchmark on adaptive regulation - rejection of unknown/time-varying multiple narrow band disturbances. *Eur. J. Contr.*, 19(4), 237–252.

Munnig Schmidt, R., Schitter, G., and van Eijk, J. (2011). *The Design of High Performance Mechatronics*. IOS Press, Amsterdam.

Ninness, B., Gibson, S., and Weller, S. (2000). Practical aspects of using orthonormal system parameterisations in estimation problems. In *SYSID*, 463–468. Santa Barbara, CA.

Ninness, B. and Hjalmarsson, H. (2001). Model structure and numerical properties of normal equations. *IEEE Trans. Circ. Syst.*, 48(4), 425.

Oomen, T., van der Maas, R., Rojas, C.R., and Hjalmarsson, H. (2014a). Iterative data-driven $\mathcal{H}_\infty$ norm estimation of multivariable systems with application to robust active vibration isolation. *IEEE Trans. Contr. Syst. Techn.*, 22(6), 2247–2260.

Oomen, T., van Herpen, R., Quist, S., van de Wal, M., Bosgra, O., and Steinbuch, M. (2014b). Connecting system identification and robust control for next-generation motion control of a wafer stage. *IEEE Trans. Contr. Syst. Techn.*, 22(1), 102–118.

Pintelon, R. and Schoukens, J. (2012). *System Identification: A Frequency Domain Approach*. Wiley-IEEE press, Hoboken, NJ, USA, second edition.

Pintelon, R. and Kollár, I. (2005). On the frequency scaling in continuous-time modeling. *IEEE Trans. Inst. Meas.*, 54(1), 318–321.

Steinbuch, M. and Norg, M.L. (1998). Industrial perspective on robust control: Application to storage systems. *Annual Reviews in Control*, 22, 47–58.

Verdult, V., Bergboer, N., and Verhaegen, M. (2002). Maximum likelihood identification of multivariable bilinear state-space systems by projected gradient search. In *Proc. CDC*, 1808. Las Vegas, NV.

van de Wal, M., van Baars, G., Sperling, F., and Bosgra, O. (2002). Multivariable $\mathcal{H}_\infty/\mu$ feedback control design for high-precision wafer stage motion. *Contr. Eng. Prac.*, 10(7), 739–755.